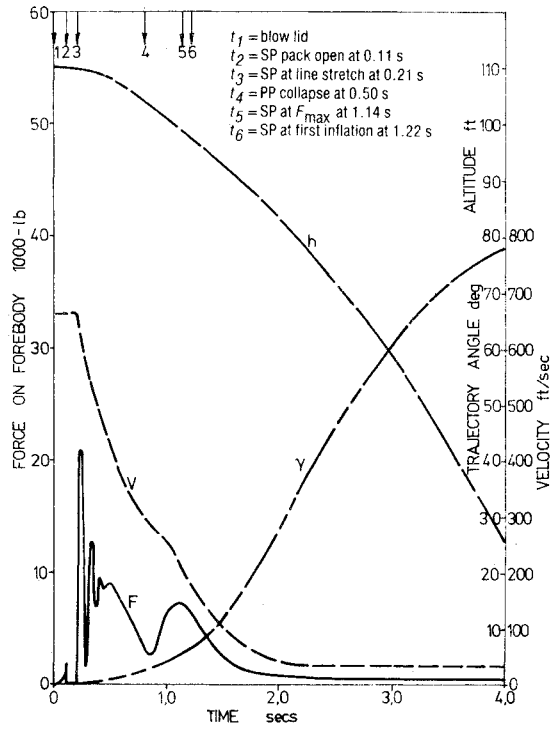

Fig. 2 Sled test of apex-attached parachute system; $M=0.6$, PP = 8 ft., SP = 26.5 ft.

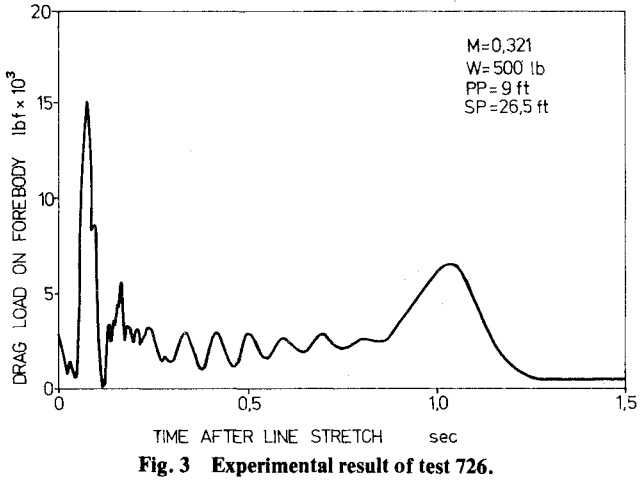

Fig. 3 Experimental result of test 726.

height h, and the trajectory angle of the forebody γ. Captions t_1 through t_5 are the event markers where $t=0$ is taken as the instant of tail can separation.

Figure 2 refers to the apex attached parachute system with the 8 ft diam primary parachute (PP) attached to the 26.5 secondary parachute (SP). Here the inflation time is 1.01 s. compared to 0.56 previously. The altitude loss has increased to 13 ft compared to 9 ft., while the peak force has fallen to 9100 lb compared to 29,700 lb previously. In principle, the force-time curves are of double peaked form for the apex-attached system, while there is only one large peak for the regular system.

Experimental Result

A number of test firings have been made on the rocket sled facility at Sandia Laboratories, Albuquerque. The object of these tests was to confirm the performance of the system described in Figs. 1 and 2. The trials undertaken so far are still in the "work-up" stage at Mach numbers around 0.3.

A typical experimental result is shown in Fig. 3 for test 726 at Mach 0.321. Here the longitudinal accelerometer record is directly related to the drag force on the forebody. The inflation time was measured at 1.25 s with a peak inflation load of only 6000 lb. The primary parachute load peaked at 15,000 lb during the initial snatch.

It should also be noted that the primary parachute tended to "breathe" at about 10 Hz in the period given by 0.3-0.8 s after the initial line stretch.

The tests conducted so far have confirmed that the large increases in the inflation time of the secondary parachute can be achieved by use of an attached apex parachute.

Conclusions

In short, it is believed that the apex attached parachute system should be investigated further. The following benefits should accrue:

1) The peak inflation loads can be reduced by a factor of 2 or 3.

2) Eliminates the use of fixed-time, conventional pyrotechnic reefing cutters.

3) The main or secondary parachute is inertially and aerodynamically reefed over the full deployment q range.

4) The canopy strength requirements are dramatically reduced. This reduction in strength should allow a replacement of ribbons by regular fabric.

5) The overall system weight should be about 40% less than the weight of a conventionally reefed ribbon parachute system. This statement takes due account of the extra weight involved in the primary parachute system.

6) No severe altitude penalty is incurred in the overall deployment.

References

[1] Wolf, D.F. and McVey, D.F., "Analysis of Deployment and Inflation of Large Ribbon Parachute," AIAA Paper 73-451, Palm Springs, Calif., 1973.

[2] Roberts, B.W., "The Aerodynamic Inflation of Shell Type, Parachute Structures," *Journal of Aircraft*, Vol. 11, July 1974, pp. 390-397.

[3] Heinrich, H.G., "Theory and Experiment on Parachute Opening Shock and Filling Time," *Proceedings of Conference on Parachutes and Related Technologies*, Royal Aeronautical Society, London, Sept. 1971.

[4] Stevens, G.W.H., "Ply-Tear Webbing as an Energy Absorber," Royal Aeronautical Society, Technical Rept. 68164, Sandia Laboratories, Alburquerque, N. Mex., 1968.

[5] Wolf, D.F., private communication, 1977.

[6] Heinrich, H.G., "Exploratory Parachute Canopy Stress Measurements During Inflation and At Steady State," AIAA Paper 75-137, Albuquerque, N. Mex., Nov. 1975.

[7] Roberts, B.W., "The Shape and Stresses in An Arbitrarily Shaped Gore Parachute Under an Arbitrary Pressure Distribution," AIAA Paper 70-1197, Dayton, Ohio, 1970.

C80-065

Note on the Yawing Moment Due to Side Slip for Swept-Back Wings

00001
00017

B. N. Pamadi* and T. G. Pai*
Indian Institute of Technology, Bombay, India

Introduction

IN Ref. 1, Babister has presented the following expression for yawing moment coefficient due to side slip for swept-

Received Aug. 9, 1979; revision received Nov. 7, 1979.

Index categories: Aerodynamics; Handling Qualities, Stability, and Control.

*Assistant Professor, Department of Aeronautical Engineering.

back wings having no dihedral,

$$C_{n\beta}=\frac{2\alpha\sin\Lambda}{Ss}\int_0^{s\sec\Lambda}(C_{Ll}-C_{D\alpha l})C_h h\,dh \tag{1}$$

In deriving the above expression, he has assumed the strip theory. However, a close examination of this reveals that he has not taken into account the relative change in thl normal dynamic pressure over the wings due to side slipping motion as shown in Fig. 1. He has considered only the relative change in the wing incidences consequent to side slipping motion and ignored the relative change in dynamic pressures. Surprisingly, this point does not seem to have been noticed so far by, for example, the Engineering Science Data Sheets,[2] USAF Stability and Control Datcom,[3] or even the more recent work by Roskam.[4] It appears that, as Roskam has stated, it is conservative to ignore the wing contribution to $C_{n\beta}$ in general.

The object of this Note is to point out that the effect of the relative change in dynamic pressure over the wings due to side slipping flow should not be ignored. This effect, as is demonstrated in this Note with the help of a numerical example, can be quite large, particularly for highly swept-back wings.

Derivation of Expression for $C_{n\beta}$

Let us consider an untapered, untwisted swept-back wing ADFCBE with no dihedral, the quarterchord line being swept back at an angle Λ. Let α be the angle of attack of the root chord. The angle of attack of a chordwise strip RT of the starboard wing, perpendicular to the quarterchord line is given by,[1]

$$\alpha_h=\alpha\sec\Lambda/(1+\beta\tan\Lambda) \tag{2}$$

The component of force along the chord RT,

$$dF=dL\sin(\alpha_s-\alpha_h)+dD\cos(\alpha_s-\alpha_h) \tag{3}$$

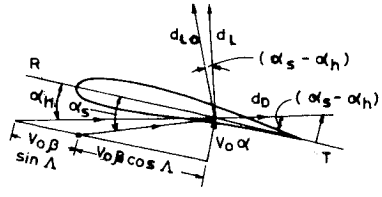

FORCES ON STRIP RT

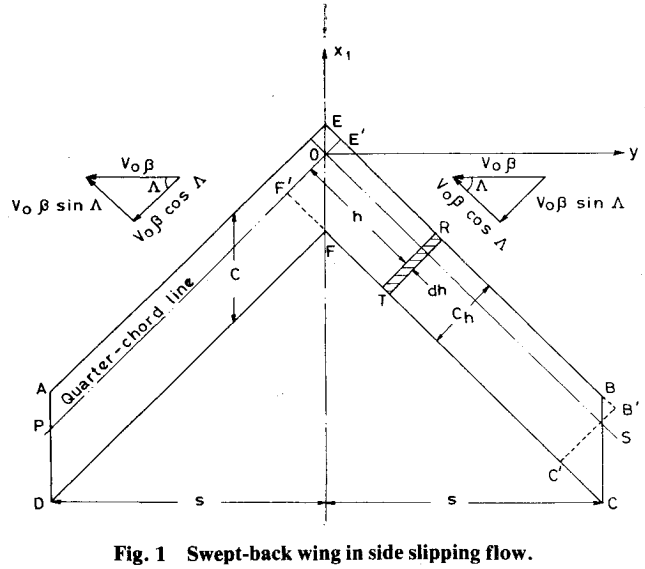

Fig. 1 Swept-back wing in side slipping flow.

where $\alpha_s=\alpha\sec\Lambda$, the local incidence of strip RT in equilibrium flight.

The normal dynamic pressure over the starboard wing is equal to

$$\tfrac{1}{2}\rho V_0^2\cos^2\Lambda(1+\beta\tan\Lambda)^2 \tag{4}$$

$$\text{Then } dF=\tfrac{1}{2}\rho V_0^2\cos^2\Lambda(1+\beta\tan\Lambda)^2\left\{\frac{C_{L_\alpha}\alpha\sec\Lambda}{(1+\beta\tan\Lambda)}\right.$$

$$\left.\cdot\alpha\beta\sin\Lambda\cdot\sec^2\Lambda+C_{D0l}+C_{D\alpha l}[\alpha\sec\Lambda/(1+\beta\tan\Lambda)]\right\}C_h\,dh \tag{5}$$

where we have assumed, $\sin(\alpha_s-\alpha_h)=\alpha_s-\alpha_h=\alpha\beta\sin\Lambda\sec^2\Lambda$ and $\cos(\alpha_s-\alpha_h)=1$.

Noting that $C_{L_l}=C_{L_\alpha}\sec\Lambda$ and the induced drag coefficient, $C_{Dil}=C_{D\alpha}\alpha\sec\Lambda$, where the suffix l denotes the local value, the yawing moment of the starboard wing about the OZ axis is given by,

$$N_s=\tfrac{1}{2}\rho V_0^2\cos^2\Lambda(1+\beta\tan\Lambda)\int_0^{s\sec\Lambda}[C_{Ll}\cdot\alpha\beta\sin\Lambda\cdot\sec^2\Lambda$$

$$+C_{D0l}(1+\beta\tan\Lambda)+C_{D\alpha l}\alpha\sec\Lambda]C_h\cdot h\,dh \tag{6}$$

Similarly the yawing moment of the port wing is,

$$N_p=\tfrac{1}{2}\rho V_0^2\cos^2\Lambda(1-\beta\tan\Lambda)\int_0^{s\sec\Lambda}[C_{Ll}\cdot\alpha\beta\sin\Lambda\sec^2\Lambda$$

$$-C_{D0l}(1-\beta\tan\Lambda)-C_{D\alpha l}\alpha\sec\Lambda]C_h h\,dh \tag{7}$$

Neglecting higher order terms involving β^2, etc., the net yawing moment about the OZ axis is,

$$N=\rho V_0^2\cos^2\Lambda\int_0^{s\sec\Lambda}[C_{Ll}\alpha\beta\sin\Lambda\sec^2\Lambda+2\beta C_{D0l}\tan\Lambda$$

$$+C_{D\alpha l}\cdot\alpha\sec\Lambda\beta\tan\Lambda]C_h\,dh \tag{8}$$

or

$$C_{n\beta}=\frac{2\sin\Lambda}{Ss}\int_0^{s\sec\Lambda}[C_{Ll}\cdot\alpha+2C_{D0l}\cdot\cos\Lambda+C_{D\alpha}\cdot\alpha]C_h h\,dh \tag{9}$$

The difference between the two values of $C_{n\beta}$ as given by Eqs. (9) and (1) turns out to be

$$\Delta C_{n\beta}=C_{n\beta}-C_{n\beta}(\text{Babister})=\frac{2\sin 2\Lambda}{Ss}\int_0^{s\sec\Lambda}C_{Dl}C_h h\,dh \tag{10}$$

It can be easily verified that Babister's formula, Eq. (1), is obtained if we take the normal dynamic pressure simply equal to $\tfrac{1}{2}\rho V_0^2\cos^2\Lambda$, as mentioned earlier.

Now to illustrate that Eq. (9) should give a value of $C_{n\beta}$ closer to the wind tunnel measurements than given by Eq. (1), the following numerical data are taken from Schlichting and Truckenbrodt.[5] This wing nearly complies with all the assumptions made earlier.

The spanwise variation of lift coefficient derived from lifting surface theory is also given for the following wing in this reference:

$\Lambda=45$ deg (no taper)
Aspect ratio = 5.0, wing section: NACA 0012
$\alpha_{stall}=18$ deg, $C_{L\max}=0.90$
$C_{L\alpha}=3.0/\text{rad}$
$C_{n\beta}=0.235\,C_L^2$

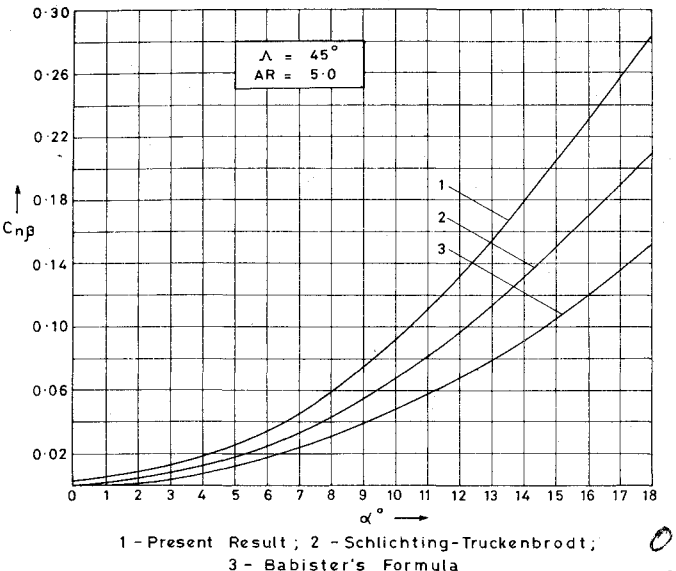

Fig. 2 Variation of $C_{n\beta}$ with α.

The results of calculations are presented in Fig. 2. In the calculations, the local angle of attack of chordwise strip RT which is taken in Eq. (3) as α sec Λ was replaced by (α sec$\Lambda - \alpha_i$) where α_i is the local induced angle of attack determined from the following relation,

$$C_{Ll} = C_{L\alpha 0}(\alpha \sec\Lambda - \alpha_i) \tag{11}$$

where $C_{L\alpha 0}$ is the two-dimensional sectional lift curve slope, which for the NACA 0012 ($C_{D0l} = 0.006$) wing section equals 0.11 per degree.[6] Also,

$$C_{Dil} = C_{D\alpha} \cdot \alpha \sec\Lambda = C_{L_l}\alpha_i \tag{12}$$

From Fig. 2 we observe that the difference between the present calculation and the experimental data[5] increases with angle of attack. A possible explanation for this deviation is as follows. In addition to the inherent limitations of the strip theory, the viscous effects ignored in the calculation become predominent at high angles of attack. As the stall propagation for a swept-back wing is from tip to root, the outboard regions which generate significant yawing moment become progressively ineffective as the angle of attack increases. Thus it is obvious that the present calculations compare better with experimental data than Babister's result, which ignores the relative change in dynamic pressure over the wings in side slip. For this wing ($\Lambda = 45$ deg), the contribution of this dynamic pressure effect to $C_{n\beta}$ is of the same order of magnitude as the other term considered by Babister. Further, it is interesting to note that even zero lift drag makes a contribution to $C_{n\beta}$, indicating that some positive directional stability can be expected from swept-back wings even under cruise condition when lift coefficient is small but the dynamic pressure is large. For higher sweep-back angles, this effect can be much more as shown by Eq. (9) and quite beneficial to the pilot while flying at high lift coefficients under cross wind conditions.

We have shown that the terms not considered by Babister are important and their contribution to wing $C_{n\beta}$ is quite significant. However, the method of computing $C_{n\beta}$ used in the above numerical example can be considerably improved by using more refined approaches such as the vortex lattice method with leading edge or side force suction analogies.

References

[1] Babister, A.W., *Aircraft Stability and Control*, Pergamon Press, New York, 1961, pp. 348-358.

[2] *Engineering Science Data Sheets*, Vol. 3, Aerodynamics, Royal Aeronautical Society, London, 1973, p. A07.01.00.

[3] Hoak, D.E., Ellison, D.E., et al., *USAF Stability and Control Datcom*, Air Force Flight Dynamics Laboratory, Flight Division, Wright Patterson Air Force Base, Ohio.

[4] Roskam, J., "Methods for Estimating Stability and Control Derivatives of Conventional Subsonic Airplanes," University of Kansas, Lawrence, Kansas, 1977, p. 7.5.

[5] Schlichting, H. and Truckenbrodt, E., *Aerodynamik des Flugzeuges*, Vol. 2, Springer Verlag, Heidelberg, 1969, pp. 70-71, 97.

[6] Abbott, I.H. and Von Doenhoff, A.E., *Theory of Wing Sections*, McGraw Hill, New York, 1949.

Boundary Layer Controls on the Sidewalls of Wind Tunnels for Two-Dimensional Tests

Y. Y. Chan*
National Aeronautical Establishment, Ottawa, Canada

Introduction

In transonic wind tunnel tests of a two-dimensional airfoil, the growth of the side wall boundary layer and its interaction with the inviscid external flow distorts the spanwise uniformity of the flow across the model and consequently induces errors in the measurements. To lessen the sidewall boundary layer effect, the common practice is to suck off the boundary layer or reduce its thickness ahead of the model. It is hoped that the newly developed boundary layer would be more energetic and therefore cause less trouble in the interaction with the inviscid flow. This method is not very effective and will be discussed further in this Note.

A more effective way to control the growth of the boundary layer is to apply suction at an area of the wall where the model is mounted. The boundary layer at that area is strongly affected by the large pressure gradients induced by the airfoils and the variation of the boundary layer thickness is the greatest. This method is employed in the NAE two-dimensional test facility.[1] In the test section of the tunnel an area of the side walls at which the model is mounted has surfaces made of porous material through which the boundary layer is bled. Because of the large resistance of the porous material, the suction velocity is nearly constant at the whole suction area and is only slightly affected by the pressure variation around the model. The amount of suction can be adjusted until the flow over the portion of the model joining the side wall is parallel to the side wall, and a spanwise uniform two-dimensional condition is established. The optimal condition of suction is determined by observing the flow visualization on the model surface and confirmed by a direct calculation of the boundary layer development on the side wall. In practice, it has been shown that in transonic testing conditions, a nominal suction velocity v_s/u_e of 0.005 is adequate for models at maximal lift coefficient. Slight oversuction has no appreciable effects on the flow pattern or the force and pressure measurements. Thus this value is then used for all testing conditions.[1]

Received July 10, 1979; revision received Dec. 10, 1979.

Index categories: Testing, Flight and Ground; Transonic Flow.

*Senior Research Officer, High Speed Aerodynamics Laboratory. Member AIAA.